Remote Sensing Letters

ISSN: 2150-704X (Print) 2150-7058 (Online) Journal homepage: http://www.tandfonline.com/loi/trsl20

Fusion of polarimetric and texture information for urban building extraction from fully polarimetric SAR imagery

Wei Zhai, Huanfeng Shen, Chunlin Huang & Wansheng Pei

To cite this article: Wei Zhai, Huanfeng Shen, Chunlin Huang & Wansheng Pei (2016) Fusion of polarimetric and texture information for urban building extraction from fully polarimetric SAR imagery, Remote Sensing Letters, 7:1, 31-40, DOI: 10.1080/2150704X.2015.1101179

To link to this article: http://dx.doi.org/10.1080/2150704X.2015.1101179

REMOTE SENSING LETTERS, 2016
VOL. 7, NO. 1, 31–40
http://dx.doi.org/10.1080/2150704X.2015.1101179

Taylor & Francis
Taylor & Francis Group

Fusion of polarimetric and texture information for urban building extraction from fully polarimetric SAR imagery

Wei Zhai[a,b,c,d], Huanfeng Shen[e], Chunlin Huang[a,d] and Wansheng Pei[c]

[a]Key Laboratory of Remote Sensing of Gansu Province, Cold and Arid Regions Environmental and Engineering Research Institute, Chinese Academy of Sciences, Lanzhou, China; [b]Gansu Earthquake Administration, Lanzhou, China; [c]College of Resources and Environment, University of Chinese Academy of Sciences, Beijing, China; [d]Heihe Remote Sensing Experimental Research Station, Cold and Arid Regions Environmental and Engineering Research Institute, Chinese Academy of Sciences, Lanzhou, China; [e]School of Resource and Environmental Sciences, Wuhan University, Wuhan, China

ABSTRACT

Building extraction from remote sensing images is very important in many fields, such as urban planning, land use investigation, damage assessment, and so on. In polarimetric synthetic aperture radar (PolSAR) imagery, the buildings not only have typical polarimetric features but also have rich texture features. In this paper, the texture information is introduced to improve the accuracy of urban building extraction from PolSAR imagery by a new method called *cross reclassification*. Based on this method, the polarimetric information-based results and texture-based results can be effectively fused. The experimental results of three representative PolSAR images with different characteristics demonstrate the effectiveness of the proposed method, and the accuracy of building extraction can be improved, compared with the traditional method using only polarimetric information.

ARTICLE HISTORY
Received 23 June 2015
Accepted 19 September 2015

1. Introduction

Buildings are the most basic living place for human beings in modern society. The automatic identification and accurate extraction of building information from remote sensing images is, therefore, important in many fields, such as the investigation and evaluation of disasters, urban planning, population estimation (Stasolla and Gamba 2008), the establishment and update of geographic information databases, land use investigation, and so on. The extraction of the building information is also a requirement for the relevant planning departments and evaluation entities. In addition, the extraction of the building information is a significant academic issue. Consequently, the study of the extraction of building information has both practical significance and value to society.

Building interpretation from high-resolution optical remote sensing images is intuitive (Dahiya, Garg, and Jat 2013; Turker and Koc-San 2015) but is vulnerable to the limitation of sunlight illumination. Synthetic aperture radar (SAR) remote sensing has unique advantages of all-time and all-weather imaging. SAR images are particularly useful when weather conditions are not suitable for optical sensing (Chen and Sato 2013). There have been

CONTACT Chunlin Huang huangcl@lzb.ac.cn

many studies of building extraction from SAR images, most of which have used multisource/multitemporal data (Gamba, Houshmand, and Saccani 2000; Tupin and Roux 2003; Zhu, Fan, and Shao 2006) and have used high-resolution (HR) single-polarization SAR images (Dong et al. 2011; Zhao, Zhou, and Kuang 2013; *Cao et al.* 2014). Only using a single SAR image without registration is more convenient and practical than using multisource/multitemporal data. Bright lines and areas with regular shape are the major characteristics of buildings in HR SAR images; however, because such details are susceptible to speckle noise, many HR SAR images may not present accurate building shapes. Compared to single or partial polarization modes (Chen and Sato 2013), fully polarimetric techniques can better assist with the understanding of scattering mechanisms and can provide much more information.

Polarimetric synthetic aperture radar (PolSAR) images not only include polarimetric information but also include texture information. If the two kinds of information are combined and effectively exert their respective superiorities, the image information comprehension ability will be improved. At present, PolSAR images are used to extract buildings mainly using the polarimetric information (Bhattacharya and Touzi 2012; Kajimoto and Susaki 2013; Yang et al. 2014). However, the texture information can provide rich image details and is very important for building recognition. To the best of our knowledge, texture information for building extraction has been mainly used in single-polarization SAR images, and both texture features and polarimetric features together are rarely considered in PolSAR images. Therefore, in this paper, the texture information is introduced, and a new method named *cross reclassification* is proposed for the fusion of polarimetric and texture information during unsupervised classification, so as to extract buildings more accurately and reliably.

2. Methodology

This research is aimed at improving building extraction accuracy through the fusion of polarimetric and texture features. The dominant ideology of the method proposed in this paper is that buildings can be regarded as a kind of typical ground object and are extracted after the typical ground objects have been classified. The whole processing chain (Figure 1) consists of three major steps: firstly, *H*/*α*/*A*-Wishart unsupervised classification of the preprocessed PolSAR data is implemented, and 16 classes are merged into three classes according to the *agglomerative hierarchical clustering* method based on minimum dissimilarity. Secondly, the span image is extracted and their grey-level co-occurrence matrix (GLCM) texture features are computed, which is defined as the total backscattering power of three scattering mechanisms. And then the unsupervised classification is performed on the group of these texture features. Thirdly, the *cross reclassification* scheme is employed to fuse the two unsupervised classification results. Finally, the buildings are extracted from the fusion results. In this way, the *cross reclassification* method effectively uses both the polarimetric information and the texture information in the PolSAR images.

The number of classes of the typical ground objects in PolSAR images differs according to the different images. In Figure 1, three kinds of typical ground objects are taken as an example in accordance with the experimental data used in this paper.

2.1. *Unsupervised classification based on polarimetric characteristics*

H/*α*/*A*-Wishart (Pottier 1998; Pottier and Lee 2000) is a classical unsupervised classification algorithm for PolSAR data. Entropy *H*, scattering mechanism angle *α* and anisotropy

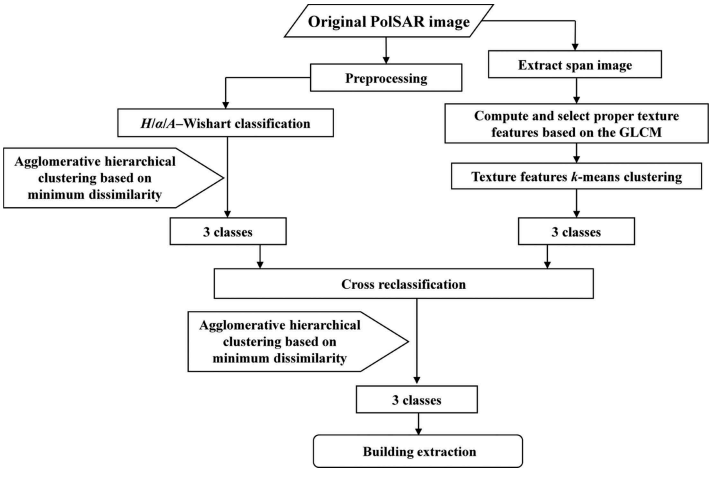

Figure 1. Framework of building extraction through the fusion of polarimetric and texture information.

A represent the randomness of target scattering, average scattering mechanism and the dominant degree of the two subordinate scattering mechanism, respectively. The eight classes obtained from the *H*/*α* plane are subdivided into 16 classes by anisotropy *A*. *H*/*α*/*A* mainly provides the polarimetric information but contains no texture information. In the experimental data used in this study, there were three classes of typical ground objects. Hence, the 16 classes produced by *H*/*α*/*A*-Wishart needed to be merged into three classes. The clusters with similarities are merged according to the *agglomerative hierarchical clustering* algorithm (Cao, Hong, and Wu 2008) based on the minimum dissimilarity criterion. This algorithm is a clustering algorithm that progressively decreases the number of clusters through each loop. For each iteration, the dissimilarities of all the possible pairs of clusters are calculated, and the two clusters with the minimum dissimilarity are merged to decrease the number of clusters by 1, while performing complex Wishart clustering to amend the locations of the cluster centres (Cao et al. 2007). We then turn to the next iteration. According to Conradsen et al. (2003) and Liu et al. (2013), the dissimilarity between the *i*th and *j*th classes can be defined as

$$D(S_i, S_j) = (N_i + N_j)\ln|\Sigma| - \left(N_i \ln|\Sigma_i| + N_j \ln|\Sigma_j|\right) \tag{1}$$

where S_i and S_j represent the *i*th and *j*th classes, respectively. N_i and N_j are the numbers of samples in the *i*th and *j*th classes, respectively. Σ_i and Σ_j are the centre covariance matrices of the *i*th and *j*th classes, respectively. Σ is the centre covariance matrix of the new class after combining the *i*th and *j*th classes. The dissimilarity $D(S_i,S_j)$ is symmetric. If $i = j$, $D(S_i,S_j)$ has a minimum value, zero. In the process of the *m*th iteration, we calculate all the $D(S_i,S_j)$ values under the condition of $i \neq j$ and find the minimum $D(S_i,S_j)$ value. If the minimum $D(S_i,S_j)$ value corresponds to the two classes of the *a*th class and *b*th class, namely

$$D(S_a, S_b) = \min\left(D(S_i, S_j)\right) \tag{2}$$

then the *a*th and *b*th classes will be merged as a new class, the *c*th class, and the *c*th and remaining classes then form a new set of classes, which are used to perform the $(m + 1)$th iteration, and so on.

2.2. *Unsupervised classification based on texture features*

The detailed structure of ground objects can be effectively reflected in texture information. Buildings with a regular arrangement and shape show notable texture features in an image. Adding texture features can make building extraction from PolSAR images more precise. Haralick, Shanmugam, and Dinstein (1973) defined the GLCM, which is one of the best-known texture analysis methods, and also proposed 14 second-order statistical features extracted from the GLCM.

The experimental results in this study showed that the four texture features of *mean, homogeneity, dissimilarity* and *angular second moment* have good distinguishing abilities for buildings and non-buildings, and are less affected by the speckle noise of SAR data. The statistic of *mean* mainly relates to the power of image, and *homogeneity* and *angular second moment* are influenced by image homogeneity, and *dissimilarity* can measure the variation of grey-level pairs in image. If pixels are very similar, then *homogeneity* and *angular second moment* are high with a low *dissimilarity* value. The four texture features can be used to set threshold values for the initial classification and can be used for unsupervised clustering. Here, the *k*-means algorithm proposed by MacQueen (1967) is used as the clustering algorithm of the unsupervised classification. In order to retain more detailed information, we calculate the four texture features of the original span image without noise filtering, with a window size of 7×7.

In order to improve the automaticity and efficiency of the program, we calculate a statistical histogram of the samples. We then choose the mean of the top 70% of the histogram as the threshold values for the initial classification, which can effectively represent most of the samples. Meanwhile, the impact of the deviating points is also reduced. We call the mean as 'hist_mean$_{70}$'. The initial clustering centres are obtained through the threshold values setting according to hist_mean$_{70}$ of the four sensitive features selected.

The experiments in this study confirmed that this method can obtain a good initial classification result, and the convergence of the iteration is fast. The convergence condition is satisfied after just one or two iterations.

2.3. *Cross reclassification*

In order to merge the results of the *H*/*α*/*A*-Wishart classification and the unsupervised classification based on the GLCM (*GLCM-based*), we propose a new method named *cross reclassification*. The central idea of *cross reclassification* is that the classification results of the *H*/*α*/*A*-Wishart algorithm and the *GLCM-based* algorithm cross each other. That is, the classification result of one of the two algorithms is reclassified by the classification result of the other algorithm.

The process of *cross reclassification* is shown in Figure 2. H_1, H_2 and H_3 represent the first, second and third classes generated from the *H*/*α*/*A*-Wishart classification, respectively. Accordingly, G_1, G_2 and G_3 represent the first, second and third classes generated from the GLCM-based classification, respectively. m_1, m_2, m_3, m_4, m_5, m_6, m_7, m_8 and m_9 represent the classes produced by *cross reclassification*. A_1, A_2 and A_3 represent the first, second and third classes after the nine classes from *cross reclassification* are merged, respectively. H_1 is subdivided into three classes labelled as m_1, m_2 and m_3 by G_1, G_2 and G_3. The class m_1 is the cluster whose data items are labelled as the first class by both *H*/*α*/*A*-Wishart and *GLCM-based* together. That is to say, the results of the two classification methods are identical for m_1. Therefore, the class labels for m_1 have high confidence. The classification results of the

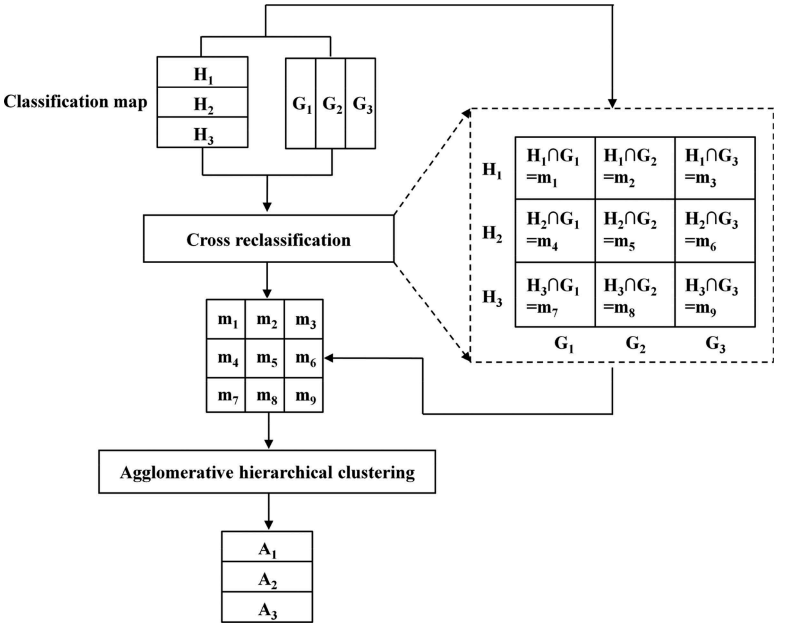

Figure 2. Diagram of the process of cross reclassification. The symbol ∩ denotes the intersection of two sets.

two methods are different for both m_2 and m_3. The cluster m_2 is the intersection of H_1 and G_2. In other words, some data items of H_1 are reclassified as the class m_2 by G_2. The data items of m_2 were classified as H_1 using the *H/α/A*-Wishart method, but were classified as G_2 using the *GLCM-based* method. In the same way, the class m_3, which is the intersection of H_1 and G_3, is identified as H_1 in the results of *H/α/A*-Wishart, but is identified as G_3 in *GLCM-based*. Analogously, H_2 is subdivided into three classes labelled as m_4, m_5 and m_6 by G_1, G_2 and G_3, and H_3 is subdivided into three classes labelled as m_7, m_8 and m_9 by G_1, G_2 and G_3.

In this way, nine classes, m_1, m_2, …, m_9, are eventually formed. That is to say, the data set is reclassified into nine classes by the *cross reclassification* method. The nine classes can then be merged into the three classes that we expect, A_1, A_2 and A_3, by reusing the *agglomerative hierarchical clustering* method described in Section 2.1, as shown in Figure 2.

In Figure 2, the diagonal elements m_1, m_5 and m_9 of the *cross reclassification* plane indicate that the classification results of the two classification methods are identical, and that the class labels for the data items of m_1, m_5 and m_9 have high confidence. When the nine classes are remerged to three classes, the pixels in m_1, m_5 and m_9 are not moved too much, and it is those in the non-diagonal elements m_2, m_3, m_4, m_6, m_7 and m_8 that are mainly moved.

If the land types are divided into n classes, the results of the two kinds of classification will cross each other to form the *cross reclassification* plane with a size of $n \times n$ according to the process described above, and we then execute agglomerative hierarchical clustering.

The method fuses the results of the two kinds of unsupervised classification and implements the fusion of the polarimetric features and texture features on the decision fusion layer, so as to make full use of the effective information of the polarimetric data. In this way, the accuracy of the two unsupervised classification methods can be improved by the use of *cross reclassification*. In the process of the merging and clustering of *cross reclassification*, other kinds of merging criteria and clustering methods could also be

chosen. This idea could also be applied to the fusion of the results generated from any other two kinds of classification method and any other category number. The classification accuracy of the two classifiers does not need to be known in advance during the implementation process. Thus, the proposed method is flexible, simple and convenient.

3. Experiments and analysis

3.1. *Experimental data*

We selected three PolSAR images of Port-au-Prince, the capital of Haiti, to undertake experiments to validate the effectiveness of the building extraction algorithm proposed in this paper. The three images cut from one large PolSAR image had different building distribution characteristics. They were acquired in the L-band by the Uninhabited Air Vehicle Synthetic Aperture Radar (UAVSAR), which is a NASA airborne SAR system, as shown in Table 1. Because of the multilook processing, a lot of image detail information had been lost, which resulted in difficulties for the building extraction task. The three data sets were labelled as data set A, data set B and data set C, respectively. Their RGB images are shown in Figure 3, formed as a colour composite of |HH-VV| (red), |HV| (green) and |HH+VV| (blue).

The buildings in the three PolSAR images have different arrangements, distributions, densities and other characteristics. The main characteristics of the buildings in data set A are that the buildings are arranged densely and regularly, and they have notable texture features. The building targets are comparatively obvious and are only slightly affected by non-buildings. The area of data set B belongs to an area with dense buildings, which are not arranged regularly. The buildings' types are complex and various, but the building targets are relatively obvious. The buildings of data set C are low-rise and sparse, with a regular arrangement. The building targets are weak and small, but are not seriously affected by non-buildings. In order to distinguish buildings from non-buildings, the land types of the three images can be divided into three classes: buildings, vegetation, and water and flat ground.

3.2. *The results of the experiments*

The building extraction results are shown in Figure 4. Some reference samples for the quantitative evaluation, marked in the three ground truth maps after registration, are also shown in Figure 4. For the ground truth maps, the red building reference samples and the yellow non-building ones are listed in Table 2.

We made an accuracy evaluation for the three methods according to the ground truth reference samples shown in Figure 4. The overall accuracy (OA) and the misclassification rate of buildings and non-buildings for each data set are listed in Table 3. The ratio of the samples which are actually buildings misclassified as non-buildings to the total number of samples of buildings is defined as the *building misclassification rate* (BMR). The ratio of the samples which

Table 1. Information about the UAVSAR data sets of this work.

Date	Flight direction	Illumination direction	Incidence angle	Number of looks	Flight altitude (m)	Spatial resolution (m)
27 January 2010	From top to bottom	Left	57°	3 (range); 12 (azimuth)	12,494	0.60 (range); 1.67 (azimuth)

Source: The reference URL is http://uavsar.jpl.nasa.gov/science/documents/.

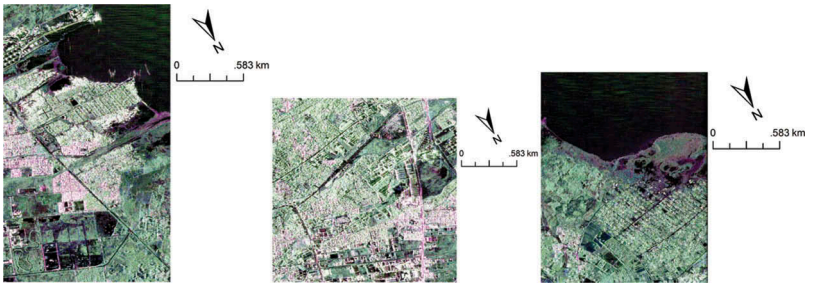

(*a*) Dataset A (*b*) Dataset B (*c*) Dataset C

Figure 3. RGB composite images of the three data sets using Pauli matrix components: |HH-VV|(red), |HV| (green) and |HH+VV|(blue) for separating the double bounce, cross pol and surface scattering. The three data sets are shown the areas of Port-au-Prince, the capital of Haiti. The centre coordinates of the images (*a*), (*b*) and (*c*) are '18°34′54″ N, 72°19′52″ E', '18°33′ 52″N, 72°19′27″ E' and '18°35′ 49″N, 72°20′ 14″E', respectively.

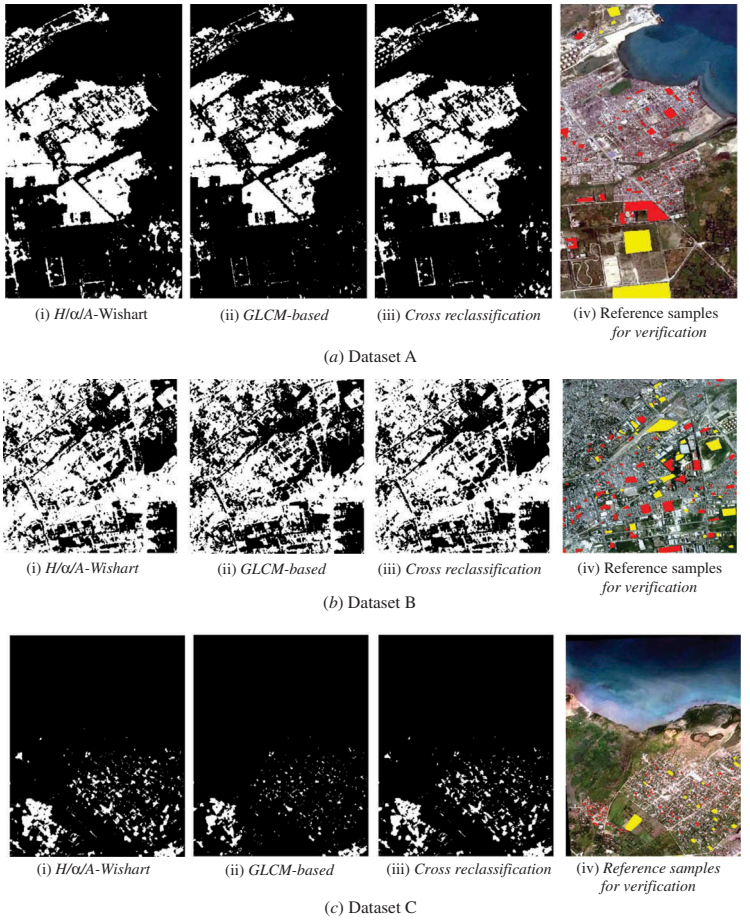

Figure 4. The results of the building extraction using the methods of *H*/*α*/*A*-Wishart, *GLCM-based* and *cross reclassification*, and the ground truth maps after registration containing the reference samples for verification. In the results of the building extraction, the white represents the building areas, and the black areas are the non-buildings. In the images of the reference samples for verification, red represents the buildings and the yellow areas are the non-buildings.

Table 2. The ground truth reference samples.

Data set	Buildings (no. of pixels)	Non-buildings (no. of pixels)
A	4354	4263
B	6701	5036
C	1020	1073

Table 3. Comparison of the results of the three classification methods for the three data sets.

	Cross reclassification			H/α/A-Wishart			GLCM-based		
Data set	OA (%)	BMR (%)	NBMR (%)	OA (%)	BMR (%)	NBMR (%)	OA (%)	BMR (%)	NBMR (%)
A	86.5	23.2	3.7	84.4	23.5	7.6	82.9	32.8	1.1
B	81.0	24.4	11.7	75.7	25.6	22.4	74.4	37.6	9.7
C	80.0	36.4	4.4	70.4	56.8	3.7	60.7	79.0	1.6

Note: OA, BMR and NBMR represent overall accuracy, the building misclassification rate and the non-building misclassification rate, respectively.

are supposed to be non-buildings misclassified as buildings to the total number of samples of non-buildings is defined as the *non-building misclassification rate* (NBMR).

As reflected in Table 3, the OA, BMR and NBMR of each data set after fusion are improved, but the magnitude of improvement for the different data sets is different. Compared with the traditional *H*/*α*/*A*-Wishart method, after using the *cross reclassification* method, the OA of data set A is increased by 2.1%, the OA of data set B is increased by 5.3% and the OA of data set C is increased by 9.6%. That is, the proposed method shows the best improvement for data set C. This shows that the proposed method is more effective for areas with a sparse building distribution and significant building texture features.

3.3. *Analysis and discussion*

Here, the misclassification of the *cross reclassification* method is analysed. For data set A, the buildings are comparatively concentrated and show a regular distribution. The densely arranged flat-roof buildings cause many flat roofs to be collected into large flat roofs, which results in these buildings being easily misidentified as flat ground. Data set B is located in a busy urban area, and the buildings are very dense and the ground layout is complex. The main reason for the misclassification is again that the flat-roof buildings are not correctly extracted. The non-buildings are mainly roads and the intervals between buildings, and there are few large areas of flat land. Therefore, the areas of non-buildings in the image are so small as to be difficult to recognize. Because of the side-looking imaging system of SAR and the fact that most of the non-buildings are very small targets, the non-buildings are often concealed by buildings. As a result, the *NBMR* of data set B is higher than for data set A. In data set C, most of the buildings with a sparse arrangement are low-rise. The multilook processing of the original data results in the building targets being very weak, and their characteristics are not obvious, so that the buildings are difficult to identify. Thus, the *BMR* of data set C is high. However, there are very few areas of tall and dense vegetation in data set C, so the NBMR is lower.

In general, the main reason for the misclassification is that the large areas of flat roofs and some low-rise buildings which are very weak targets are easily misclassified as non-buildings. The major reason for the high *NBMR* is that some non-buildings are hidden. The *cross reclassification* method is proposed for the effective fusion of the polarimetric and texture features by combining the results of the two unsupervised classification methods. In the application of urban building extraction, it can achieve the aim of improving the

extraction accuracy, especially for the buildings with significant texture features. However, the effect of the proposed method in other applications remains to be verified.

4. Conclusion

Even in the same area the ground features of different parts or different blocks may be different. Especially for urban areas urban layout is not limited to one style and the buildings are often diverse. Thus, when extracting buildings of a large area from an image, we should first divide the study area into subareas based on their similarity and then extract the buildings from these subareas.

In this work, the effective fusion of the polarimetric and texture information is achieved by *cross reclassification*, and the accuracy of the building extraction is improved. Three PolSAR images with different characteristics were selected for the verification of the proposed method. The experimental results showed that the accuracy of each data set after fusion was improved, but the amount of improvement for the different data sets was different. The proposed method is more effective for images in which the buildings have significant texture features. If the buildings are sparsely and regularly arranged, and the image intensity of the buildings is low, then the accuracy of the building extraction will be effectively improved by adding the texture features to the polarimetric features using the *cross reclassification* method. For dense buildings with comparatively high image intensity, the polarimetric information can be used to extract buildings with a comparatively high degree of accuracy, so the improvement in the extraction accuracy is relatively small. In the process of classification, the misclassification is caused by: (1) because of the multilook processing of the original data, a great deal of edge and corner information of the buildings is lost, which results in the characteristics of some buildings being unclear and some low-rise building targets being very weak; (2) the processing window prevents some small single buildings being recognized; and (3) some non-buildings with linear and planar shapes in the image are easily concealed.

Disclosure statement

No potential conflict of interest was reported by the authors.

Funding

This work was supported by the Major State Basic Research Development Program [grant number 2011CB707103]; the Hundred Talent Program of the Chinese Academy of Sciences [grant number 29Y127D01]; and the Cross-disciplinary Collaborative Teams Program for Science, Technology and Innovation of the Chinese Academy of Sciences.

References

Bhattacharya, A., and R. Touzi. 2012. "Polarimetric SAR Urban Classification Using the Touzi Target Scattering Decomposition." *Canadian Journal of Remote Sensing* 37 (4): 323–332. doi:10.5589/m11-042.

Cao, F., W. Hong, and Y. Wu. 2008. "An Unsupervised Classification for Fully Polarimetric SAR Data Using Cloude-Pottier Decomposition and Agglomerative Hierarchical Clustering Algorithm." *Acta Electronica Sinica* 36 (3): 543–546.

Cao, F., W. Hong, Y. Wu, and E. Pottier. 2007. "An Unsupervised Segmentation with an Adaptive Number of Clusters Using the Span/H/α/A Space and the Complex Wishart Clustering for Fully

Polarimetric SAR Data Analysis." *IEEE Transactions on Geoscience and Remote Sensing* 45 (11): 3454–3467. doi:10.1109/TGRS.2007.907601.

Cao, Y., C. Su, and G. Yang. 2014. "Detecting the Number of Buildings in a Single High-Resolution SAR Image." *European Journal of Remote Sensing* 47: 513–535. doi:10.5721/EuJRS20144729.

Chen, S.-W., and M. Sato. 2013. "Tsunami Damage Investigation of Built-Up Areas Using Multitemporal Spaceborne Full Polarimetric SAR Images." *IEEE Transactions on Geoscience and Remote Sensing* 51 (4): 1985–1997. doi:10.1109/TGRS.2012.2210050.

Conradsen, K., A. A. Nielsen, J. Schou, and H. Skriver. 2003. "A Test Statistic in the Complex Wishart Distribution and Its Application to Change Detection in Polarimetric SAR Data." *IEEE Transactions on Geoscience and Remote Sensing* 41 (1): 4–19. doi:10.1109/TGRS.2002.808066.

Dahiya, S., P. K. Garg, and M. K. Jat. 2013. "Object Oriented Approach for Building Extraction from High Resolution Satellite Images." In *2013 IEEE 3rd International Advance Computing Conference (IACC)*, 1300–1305. Ghaziabad: IEEE.

Dong, Y., H. Chen, D. Yu, Y. Pan, and J. Zhang. 2011. "Building Extraction from High Resolution SAR Imagery in Urban Areas." *Geo-spatial Information Science* 14 (3): 164–168. doi:10.1007/s11806-011-0525-9.

Gamba, P., B. Houshmand, and M. Saccani. 2000. "Detection and Extraction of Buildings from Interferometric SAR Data." *IEEE Transactions on Geoscience and Remote Sensing* 38 (1): 611–617. doi:10.1109/36.823956.

Haralick, R. M., K. Shanmugam, and I. H. Dinstein. 1973. "Textural Features for Image Classification." *IEEE Transactions on Systems, Man and Cybernetics* 6: 610–621. doi:10.1109/TSMC.1973.4309314.

Kajimoto, M., and J. Susaki. 2013. "Urban-Area Extraction from Polarimetric SAR Images Using Polarization Orientation Angle." *IEEE Geoscience and Remote Sensing Letters* 10 (2): 337–341. doi:10.1109/LGRS.2012.2207085.

Liu, B., H. Hu, H. Wang, K. Wang, X. Liu, and W. Yu. 2013. "Superpixel-Based Classification with an Adaptive Number of Classes for Polarimetric SAR Images." *IEEE Transactions on Geoscience and Remote Sensing* 51 (2): 907–924. doi:10.1109/TGRS.2012.2203358.

MacQueen, J. 1967. "Some Methods for Classification and Analysis of Multivariate Observations." *Proceedings of the Fifth Berkeley Symposium on Mathematical Statistics and Probability* 1 (14): 281–297.

Pottier, E. 1998. "Unsupervised Classification Scheme and Topography Derivation of Polsar Data Based on the H/α/A Polarimetric Decomposition Theorem." Proceedings of the 4th International Workshop on Radar Polarimetry, Nantes, July 13.

Pottier, E., and J. S. Lee. 2000. "Application of the «H/A/alpha» Polarimetric Decomposition Theorem for Unsupervised Classification of Fully Polarimetric SAR Data Based on the Wishart Distribution." *In SAR Workshop: CEOS Committee on Earth Observation Satellites* 450: 335–335.

Stasolla, M., and P. Gamba. 2008. "Spatial Indexes for the Extraction of Formal and Informal Human Settlements from High-Resolution SAR Images." *IEEE Journal of Selected Topics in Applied Earth Observations and Remote Sensing* 1 (2): 98–106. doi:10.1109/JSTARS.2008.921099.

Tupin, F., and M. Roux. 2003. "Detection of Building Outlines Based on the Fusion of SAR and Optical Features." *ISPRS Journal of Photogrammetry and Remote Sensing* 58 (1–2): 71–82. doi:10.1016/S0924-2716(03)00018-2.

Turker, M., and D. Koc-San. 2015. "Building Extraction from High-Resolution Optical Spaceborne Images Using the Integration of Support Vector Machine (SVM) Classification, Hough Transformation and Perceptual Grouping." *International Journal of Applied Earth Observation and Geoinformation* 34: 58–69. doi:10.1016/j.jag.2014.06.016.

Yang, W., X. Yin, H. Song, Y. Liu, and X. Xu. 2014. "Extraction of Built-up Areas From Fully Polarimetric SAR Imagery Via PU Learning." *IEEE Journal of Selected Topics in Applied Earth Observations and Remote Sensing* 7 (4): 1207–1216. doi:10.1109/JSTARS.4609443.

Zhao, L., X. Zhou, and G. Kuang. 2013. "Building Detection from Urban SAR Image Using Building Characteristics and Contextual Information." *EURASIP Journal on Advances in Signal Processing 2013* 1: 1–16.

Zhu, J. J., X. T. Fan, and Y. Shao. 2006. "Building's Roof Extraction by Fusing High-Resolution SAR with Optical Images." *Journal of the Graduate School of the Chinese Academy of Sciences* 23 (2): 178–185.